Stable carbon isotope discrimination by human 3-hydroxy-3-methylglutaryl-coenzyme A reductase

Svena M. Lüdke,[1,*] Ulrich Flenker,[*] Wilhelm Schänzer,[*] and Dietmar Schomburg[†]

Institute of Biochemistry,* German Sport University Cologne, Am Sportpark Müngersdorf 6, 50933 Cologne, Germany; and Institute for Biochemistry and Biotechnology,[†] Technical University Braunschweig, Langer Kamp 19B, 38106 Braunschweig, Germany

Abstract **The aim of this study was to investigate the possible existence and magnitude of stable carbon isotope discrimination by human 3-hydroxy-3-methylglutaryl-coenzyme A reductase (HMGR). The catalytic portion of HMGR was expressed and purified. The reaction product mevalonate was lactonized and extracted from the reaction mixture by a solid-phase extraction protocol. Stable carbon isotope ratios of mevalonolactone (MVL) were analyzed by gas chromatography-combustion-isotope ratio mass spectrometry. An average fractionation factor $^{12}k/^{13}k$ of 1.0031 ± 0.0004 for all carbon atoms contained in MVL was estimated by the method of internal competition. The value was calculated by nonlinear curve fitting, where the ratio $^{13}C/^{12}C$ of MVL was plotted versus the fraction of reaction.**—Lüdke, S. M., U. Flenker, W. Schänzer, and D. Schomburg. **Stable carbon isotope discrimination by human 3-hydroxy-3-methylglutaryl-coenzyme A reductase.** ***J. Lipid Res.*** **2008.** 49: **2620–2626.**

Supplementary key words mevalonate pathway • steroids • kinetic isotope effect • isotope ratio mass spectrometry • curve fitting • doping control

Kinetic isotope effects (KIEs) present in enzyme-catalyzed reactions may evidence the corresponding reaction mechanism (1) and account for the natural variation of the stable isotope signatures of biological compounds (2, 3). These parameters are of rapidly increasing interest in the geological, biological, and forensic sciences, to name but some.

The interpretation of such data will be facilitated by a sound understanding of the underlying processes. Although a perfect analysis of isotope fluxes in metabolic networks is virtually impossible (3), and purely empirical "isotope fingerprinting" is applied routinely and successfully, reliable predictors can be found and quantified from time to time. For example, lipids are typically strongly depleted in ^{13}C versus other classes of biological compounds (4). This phenomenon usually is attributed to KIEs during the decarboxylation of pyruvate (5).

Considering this phenomenon, the stable carbon isotope ratios of human steroid hormones exhibit somewhat unusual values. Steroids isotopically are only slightly lighter than carbohydrates and proteins (6). Hence, steroid biosynthesis is unlikely to be limited by pyruvate decarboxylation, and other processes must control the stable isotope ratios of steroids.

We hypothesized that owing to its key position in steroid biosynthesis, 3-hydroxy-3-methylglutaryl-coenzyme A reductase (HMGR) might play a pivotal role here. The hypothesis is supported by the observation that steroid hormones reveal stronger ^{13}C depletion when contraceptives are administered (6). This probably indicates the emergence of rate limitation resulting from feedback-induced downregulation of the enzyme. HMGR is among the most highly regulated enzymes in nature (7). The different levels of regulation include transcription, translation, enzyme degradation, and phosphorylation.

HMGR (EC 1.1.1.34) catalyzes the four-electron reduction of HMG-CoA to mevalonate and CoASH: HMG-CoA + 2 NADPH + 2 H+ → mevalonate + CoA-SH + 2 NADP+. The human enzyme assumes a rate-limiting position in the mevalonate pathway. Numerous biomolecules originate from this process, including haem, ubiquinone, and cholesterol. Besides its diverse functions in animals, the latter forms the backbone of steroid hormones.

Chemical reactions involving bond making or breaking almost always reveal normal isotope effects, which means slower reaction of the isotopically heavier isotopologues (1). Therefore, the reaction of HMGR is likely to discriminate substrate molecules with carbonyl-^{13}C vicinal to the thioester bond between the HMG and the CoA moiety (**Fig. 1**). The aim of this study was to investigate the pos-

Manuscript received 12 June 2008 and in revised form 29 July 2008.

Published, JLR Papers in Press, July 30, 2008.
DOI 10.1194/jlr.M800313-JLR200

Abbreviations: GC-C-IRMS, gas chromatography-combustion-isotope ratio mass spectrometry; HMGR, 3-hydroxy-3-methylglutaryl-coenzyme A reductase; KIE, kinetic isotope effect; MVL, mevalonolactone; T, testosterone.

[1] To whom correspondence should be addressed.
e-mail: s.luedke@biochem.dshs-koeln.de

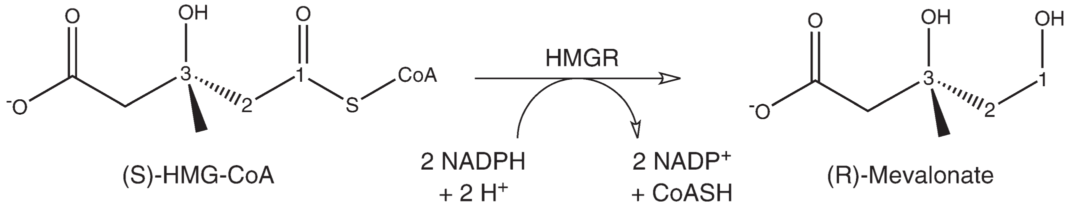

Fig. 1. Enzyme reaction of 3-hydroxy-3-methylglutaryl-coenzyme A reductase (HMGR). Isotope effects are expected at C-1, C-2, and C-3, the group of atoms adjoining the cleaved C-S bond.

sible existence and magnitude of isotope discrimination by HMGR in order to provide better understanding of the factors that control the $^{13}C/^{12}C$ ratios of sterols, steroids, and other products of the mevalonate pathway.

EXPERIMENTAL PROCEDURES

Vector design

A plasmid containing the gene for human HMGR was purchased from the American Type Culture Collection. The catalytic subunit (residues 420–888) (8) was amplified by PCR introducing an *Afl*III and *Bam*HI restriction site at the ends (restriction enzymes from New England Biolabs). The fragment was inserted into the pNHis vector (9) between the *Nco*I and *Bam*HI restriction sites using standard ligation procedures with T4 DNA ligase (Roche). The pNHis vector introduces an N-terminal polyhistidine tag that permits affinity purification. The ligation mixture was transformed into *Escherichia coli* DH5α. Vectors containing the insert were identified by agarose gel electrophoresis of minipreparations of plasmid DNA from single colonies. A suitable vector was amplified in DH5α cells (Qiagen plasmid midi kit). To avoid fragmentary expression starting from an internal translation initiation site (10), M485 was mutated to I485 by side-directed mutagenesis (reagents from NEB). According to Istvan et al. (8), the enzymatic activity of the M485I mutant protein is unchanged compared with the wild-type protein.

Protein expression and purification

For expression of the fusion protein, the vector was transformed into *E. coli* BL(DE3). Cells were grown in Luria Bertani medium (11) at 37°C until they reached an optical density at 600 nm of 0.8, then induced with 1 mM isopropyl-β-D-thiogalactoside and grown at 25°C for 4 h. Purification was carried out using an Ni-NTA Agarose affinity column (Qiagen) according to a vendor-provided protocol. Protein concentrations were determined by the method of Bradford (12). The two main fractions were combined, concentrated by centrifugal filtration (Millipore am-icon ultra 30,000), and re-buffered in potassium phosphate buffer (13) (0.2 M KCl, 0.16 M potassium phosphate, 0.004 M EDTA, and 0.01 M DTT, pH 6.8). Enzyme purity was checked by SDS-PAGE. For storage, the solution was spiked with 10% (v/v) glycerol, and aliquots of 200 μl were kept at −20°C.

Enzymatic reaction

The reaction system consisted of 160 mM potassium phosphate (pH 6.8), 200 mM KCl, 420 myM NADPH (Sigma), and 311 myM (R,S)-HMG-CoA (Fluka) in a final volume of 800 μl. The reaction was initiated by adding the enzyme to the complete assay mixture in a volume that was sufficient to complete the conversion within approximately 14 min. The HMG-CoA-dependent oxidation of NADPH was monitored at 340 nm in a spectrophotometer (Pharmacia Biotech Ultrospec 2000) equipped with a cell holder adjusted at 37°C. Up to three samples of 250 μl per run were taken and transferred into ice-cooled glass vials. The vials had been equipped with a solution of pravastatin (Sigma) to inhibit further reaction. For samples taken at fractions of reaction smaller than 0.15, volumes of 500 μl were pipetted.

Sample preparation

For lactonization of mevalonic acid, the samples volume was doubled by addition of 0.1 M HCl, and the reaction was left unattended at room temperature for about 1 h. Solid-phase extraction was conducted as described by Saini et al. (14), with slight modifications. Briefly, the samples were individually transferred to a solid-phase extraction cartridge (Separtis Isolute ENV+ 100 mg/3 ml) that had been washed and preconditioned with 3 ml methanol followed by 1 ml water. The sample was allowed to enter the column bed by gravity flow, and the column was washed with 500 μl HCl followed by 500 μl water. The cartridges were dried under gentle vacuum suction. The column bed was conditioned with 500 μl methanol, and another volume of 500 μl eluted the analytes. The methanol extract solution was dried in a vacuum dessicator over phosphorus pentoxide. For gas chromatography-combustion-isotope ratio mass spectrometry (GC-C-IRMS) analysis, analytes were taken up in individually determined volumes of tert-butyl methyl ether, in order to minimize concentration varieties.

Stable isotope analysis

Stable carbon isotope analysis of mevalonolactone (MVL) was performed by GC-C-IRMS. The hardware encompassed an Agilent GC 6890 (Agilent Technologies) coupled to a Thermo Delta-plus XP gas isotope ratio mass spectrometer. The system was largely modified as described by Flenker, Güntner, and Schänzer (15).

Briefly, the solvent removal, which is essential to GC-C-IRMS, was performed before passage of the GC column. A KAS-4 Gerstel cooled injection system supported by an auxiliary vacuum was employed for this purpose.

Solvent removal was achieved at a temperature of 5°C within an interval of 1 min. The vent flow was adjusted to 50 ml/min, and the auxiliary vacuum was set to −0.1 bar. The sample transfer to the GC column was performed at 200°C within another minute. The material was re-condensed on the column at 35°C. Subsequently, the injection port was purged at a temperature 300°C, where the gas flow was set to 100 ml/min. The temperature rates between the different steps amounted to 10 K/s.

The GC column was a Macherey and Nagel Optima-1701. The dimensions were 30 m length, 320 μm inner diameter, and 0.5 μm film thickness. The carrier gas flow was set to 1.8 ml/min, where constant flow mode was used.

The initial GC temperature (35°C) was maintained for 2 min. The temperature then was raised to 135°C at 40 K/min. Subsequently, the temperature was changed to 250°C at a rate of 10 K/min.

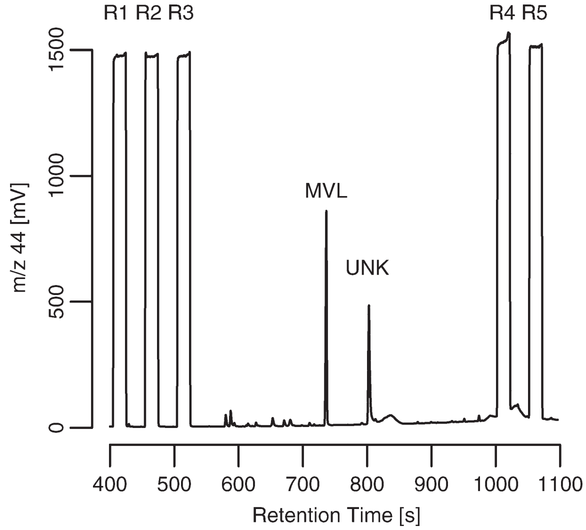

Fig. 2. Gas chromatography-combustion-isotope ratio mass spectrometry analysis of mevalonolactone (MVL) isolated from the HMGR reaction mixture. R1–R5, reference gas pulse; UNK, unkown contaminant. R3 and R5 were used to calculate the $^{13}C/^{12}C$ of MVL in this run.

Typically, two reference gas pulses were employed to calculate the $^{13}C/^{12}C$ ratio of MVL. For this purpose, one uncontaminated pulse before and one after the MVL signal were selected. **Figure 2** shows a typical analysis and illustrates the procedure. The reference gas was calibrated versus an n-alkane mixture kindly provided by the University of Indiana (16).

Data evaluation

The spectrophotometric absorbance was plotted against time. During sampling, the cover of the spectrophotometer had to be opened. Data measured within these intervals were removed from the plot. A cubic smoothing spline (17) was fitted to the remainder of the data. It was assumed that the observed decrease of NADPH concentration depended on two different factors, the consumption of NADPH during the enzyme reaction and the enzyme-independent decay of NADPH. The latter depends on pH and temperature (18).

In order to isolate the enzymatic effect, the curve was corrected by addition of the absolute difference of two decay lines. The latter were individually calculated according to the NADPH concentration before and after complete conversion of (S)-HMG-CoA, respectively. The fraction of reaction then was calculated as the ratio of the difference between initial absorbance and absorbance at the time of sampling divided by the total difference of absorbances (**Fig. 3**).

The fractionation factor (α) and the isotopic ratio of the product molecule after complete conversion (R_∞) were estimated by nonlinear least-squares curve fitting. The software was R in its latest version where the nls-library was employed (19).

The model formula was derived from the rate laws of the stable carbon isotopes (see Appendix):

$$R_t = \frac{1 - \exp(\log(1 - f)/\alpha)}{f} \cdot R_\infty \qquad (Eq.\ 1)$$

R_t is the isotopic ratio of the sample at time t and f is the corresponding fraction of reaction.

The KIE of the enzyme reaction is then given by

$$\text{KIE} = (\alpha - 1) = (^{12}k/^{13}k) - 1, \qquad (Eq.\ 2)$$

where ^{12}k and ^{13}k indicate the rate constants for ^{12}C and ^{13}C, respectively.

RESULTS AND DISCUSSION

Figure 2 shows a typical GC-C-IRMS analysis of MVL following our protocol for enzymatic production, sample preparation, and $^{13}C/^{12}C$ analysis.

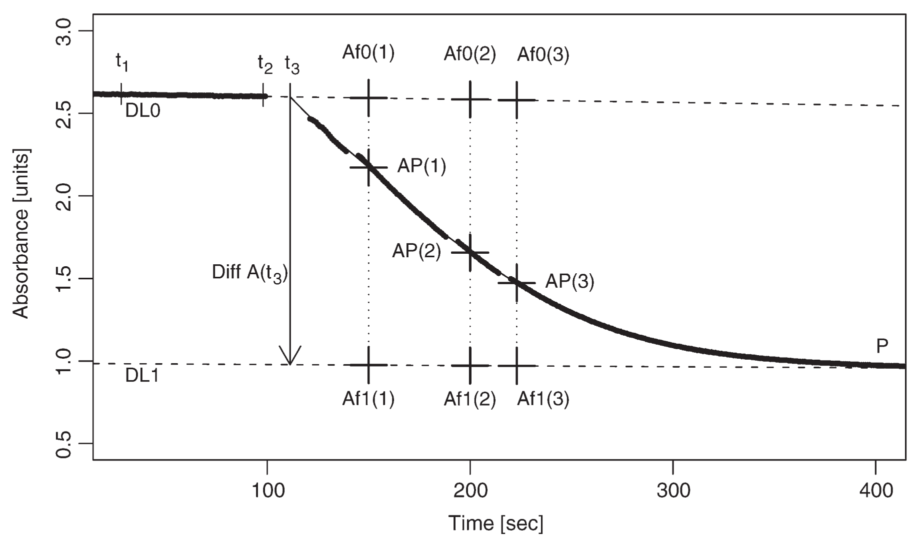

Fig. 3. Determination of the fraction of reaction f from spectrophotometric data. Decay lines DL0 and DL1: estimated enzyme independent change of absorbance for $f = 0$ and $f = 1$, respectively; Curve P: cubic smoothing spline fitted to absorbance data; t_1 to t_2: interval evaluated for linear regression and calculation of DL0; t_3: enzyme addition; Diff A(t_3): difference of absorbance due to complete conversion of (S)-HMG-CoA; AP(x): absorbance of sample x; Af0: assumed absorbance for $f = 0$; Af1: assumed absorbance for $f = 1$; Fraction of reaction of sample x: $f = (\text{AP - Af0})/(\text{Af1 - Af0})$.

In this case, the reference gas pulses R3 and R5 were employed to calculate the $^{13}C/^{12}C$ of MVL. The contamination of R4 appeared irregularly and probably results from the solid-phase extraction. The MVL signal itself is clearly resolved and certainly yields valid results. Because the HMGR reaction was stopped after varying intervals, the resulting MVL concentrations were rather different. The required amounts of solvent, however, were estimated in advance, and thus, approximately identical peak heights could be obtained. In fact, these varied by less than a factor of 3, which falls well within the linear dynamic range of IRMS analyses.

Figure 4 shows the observed relation between f and R_t. The fitted curve according to equation 1 is plotted. Analysis of the residuals suggested presence of some outliers. In fact, two outliers were confirmed by Huber statistics (20). The curve was refitted after removal of these points. The corresponding estimates for α, R_∞, and the calculated KIE are listed in **Table 1**.

The standard deviation of the residuals is close to the known repeatability precision of GC-C-IRMS analyses. Moreover, the residuals are independent from f and exhibit random scatter. It can therefore be assumed that the relation between R and f is described adequately.

Both estimates for α and R_∞ and their corresponding confidence intervals could be confirmed by application of bootstrap methods (21).

KIEs are commonly determined (22–24) by the method of internal competition (1). The calculation employs the equation proposed by Tong and Yankwich (25) or its simplified version by O'Leary (26), both describing α in terms of f, R_t, and R_∞. This method requires several measurements of the isotopic composition R_t of the starting material or the reaction product over the range from as little as

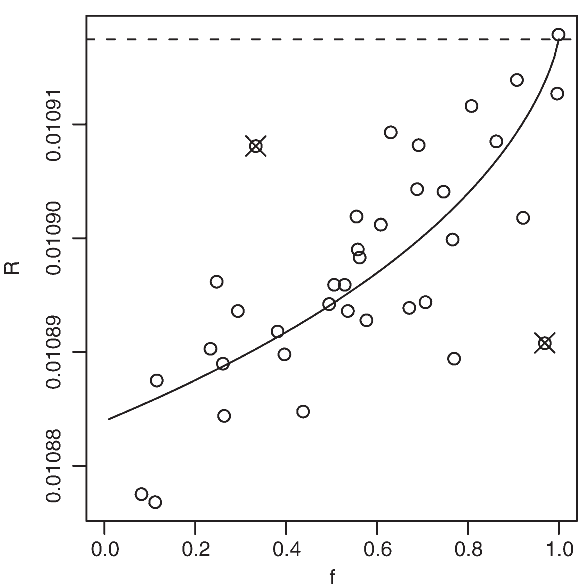

Fig. 4. Observed relationship between $R = {}^{13}C/{}^{12}C$ of MVL and the fraction of reaction f. Two outliers plotted as crossed points were removed from the dataset. The dashed line marks the value of R_∞.

TABLE 1. Estimates for α and R_∞.

Parameter	Estimate	SE	CI
α	1.0031	$\pm 4 \times 10^{-4}$	$\pm 8 \times 10^{-4}$
R_∞	1.0917×10^{-2}	$\pm 3 \times 10^{-6}$	$\pm 5 \times 10^{-6}$
KIE	3.1‰	±0.4‰	±0.8‰

KIE, kinetic isotope effect; SE, standard error; CI, confidence interval (95%).

1% reaction to as much as 50% reaction. Second, the value of R_∞, which is the isotopic composition of the product at total conversion, must be known.

Because of the steep dependence of the product isotopic composition at the end of the reaction (see Fig. 1), R_∞ is afflicted with large experimental errors and can be regarded as the major source of bias. However, the curve-fitting method used in this study does not require any exact value for R_∞. In fact, R_∞ and α are estimates obtained from the fitting process.

The model equation, which was used to calculate the KIE, is based upon the assumption of a pseudo first-order irreversible enzyme reaction. Human HMGR utilizes two equivalents of NADPH as a cosubstrate. In order to meet the first-order demand, limitation by a substrate other than HMG-CoA was avoided by excess NADPH.

The calculated KIE has to be treated as the average isotope effect on all carbon atoms contained in the product molecule. Assuming that the isotope effect would be largely restricted to C-1 and only normal isotope effects contribute to the observed value, the maximum expected depletion of ^{13}C at C-1 can be assessed, at least roughly. Thereto the average isotope effect is multiplied with the number of carbon atoms present in the product molecule, in this case six for MVL. The resulting value of 18.6‰ is not unusual in enzymatic reactions in which carbon bonds are cleaved. For example, bacterial decarboxylases have been reported to exhibit KIEs between 14.7‰ and 18.2‰ at C-1 (22, 26).

However, Melzer and Schmidt (5) investigated the pyruvate dehydrogenase reaction from two different organisms and calculated position-specific isotope effects. In fact, ^{13}C primary isotope effects from 9‰ to 25‰ were observed and secondary isotope effects still caused depletions around 3‰.

From the above, it is certainly inadequate to attribute the entire isotope effect of HMGR to C-1. The effect would rather show some kind of distribution between the atoms C-1, C-2, and possibly even C-3 (Fig. 1). Nonetheless, a calculated propagation of ^{13}C depletion from mevalonate to cholesterol would remain unaffected. Cholesterol incorporates all three of the carbon atoms concerned from six molecules of mevalonate. The depletion would therefore propagate with $18.6 \times 6/27 = 4.1$‰ to the C^{27}-body of cholesterol (**Fig. 5**). Likewise, pregnanes incorporate five groups of C-1 to C-3 and would show a ^{13}C depletion of about $18.6 \times 5/21 = 4.4$‰.

In contrast, androstanes incorporate C-1 and C-2 from mevalonate at equal numbers, but lack one atom C-3 (Fig. 5). The expected ^{13}C depletion of this compound

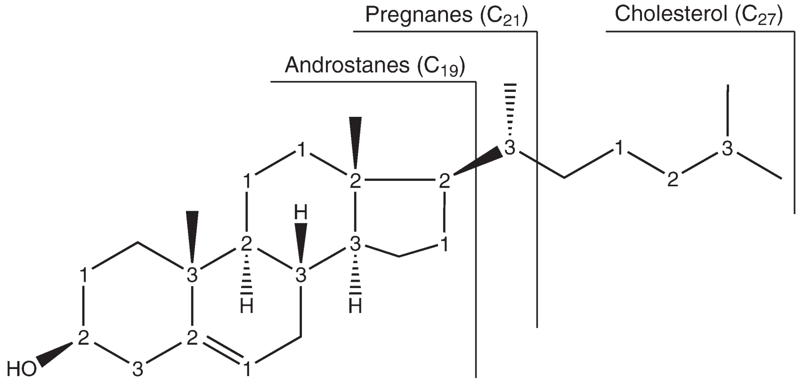

Fig. 5 Cholesterol incorporates carbon atoms C-1 to C-3 from six mevalonate molecules. The denoted positions 1 to 3 refer to the mevalonate molecule. C_{19}-steriode hormones lack the side chain and concurrently one of the C-3 atoms.

depends on the actual effect attributed to C-3. Considering it to fall between one-third and zero of the overall KIE, androstanes would exhibit depletions between $(18.6 \times 5 - 18.6/3)/19 = 4.6‰$ and $18.6 \times 5/19 = 4.9‰$, respectively. All of these numbers represent estimates that rely on sole limitation of steroid biosynthesis by HMGR.

The results are of practical relevance for doping control, where stable isotope ratios are used to identify the primary sources of steroids. The method compares the $^{13}C/^{12}C$ ratios of androgens or corresponding metabolites to those of steroids from independent pathways. For example, testosterone (T, C_{19}) may be compared with pregnanediol (C_{21}). The latter thus serves as "endogenous reference compound." Synthetic androgenic steriods betray their origin in that their $^{13}C/^{12}C$ values significantly differ from those of the endogenous reference compounds. Up to now, with very few exceptions, only ^{13}C depletions have been observed for synthetic steroids.

Consequently, during the application of synthetic T, the $^{13}C/^{12}C$ ratios of T itself and its metabolites will be reduced compared with the purely biosynthetic pregnanes. Depending on the considered target and reference compounds, a difference of at least 3‰ on the δ-scale[1] must be exceeded in order to tell the presence of synthetic steroids (28).

The described doping control methodology presumes that physiological factors do not significantly increase the corresponding differences in stable isotope composition. As demonstrated above, full limitation by HMGR could result in a maximum difference in ^{13}C depletion of $4.9 - 4.4 = 0.5‰$ when comparing C_{19}- and C_{21}-steroid hormones. Therefore ^{13}C discrimination by HMGR would only be able to slightly quench the ^{13}C enrichment attributed to doping. It can be stated that the influence of the HMGR isotope effect will not significantly exceed the analytical error generally present in GC-C-IRMS. It is unlikely that corresponding results will be corrupted by the described phenomena. Nonetheless, it should be kept in mind that different steroids, although originating from an identical pathway, do not necessarily exhibit identical stable isotope signatures. Because the atoms of mevalonate will have a nonstatistical distribution of ^{13}C, the measured average depletion depends on the atoms incorporated into or removed from the analyzed molecule.

Apart from practical issues, our results allow one to draw interesting conclusions concerning the nature of steroid biosynthesis. Crude lipids were found to be depleted in ^{13}C by 7‰ relative to biomass (4, 27). The rate limitation of acetate formation catalyzed by pyruvate dehydrogenase is likely to be responsible for this phenomenon (5). However, among lipids, FFAs exhibit considerable $^{13}C/^{12}C$ depletions of around 8‰, whereas steroids are only sightly depleted by ∼1‰, compared with biomass (6). The lack of ^{13}C depletion rules out rate limitation of steroid formation by the decarboxylation of pyruvate.

It is usually assumed that HMGR features the rate-limiting step in sterol synthesis. In the present study of the HMGR reaction, a depletion propagating with 4–5‰ to sterols has been calculated. Considering that sterols appear much less depleted than can be predicted from this result, it may be concluded that under physiological conditions, most of the HMG-CoA emerging in the relevant compartment is converted to mevalonate. This would result in the disappearance of significant HMGR-induced isotope fractionation, for the most part.

In general, the influences of in vivo isotope effects are modulated by various factors such as the branching of carbon fluxes to alternative metabolic pathways or compartmentalization. To interpret patterns of isotopic depletion, the structure and characteristics of the related network of reactions has to be considered (3). Thus, the results presented contribute to the interpretation of isotopic patterns in the mevalonate pathway.

[1] The $\delta^{13}C$ value is defined as:

$$\delta^{13}C(‰) = \left(\frac{[^{13}C]/[^{12}C]_{sample}}{[^{13}C]/[^{12}C]_{standard}} - 1\right) \cdot 1000$$

The standard is carbon dioxide from PeeDee Belemnite isotopic standard limestone (29).

APPENDIX

R_t AS A FUNCTION OF f, α, AND R_∞

We presume a system of pseudo first-order irreversible reactions of the form A → B with the rate constant k.

For molecules with different isotopic composition at positions that influence the reaction rate, we assume for the lighter carbon isotope ^{12}C and for the heavier carbon isotope ^{13}C, respectively:

$$A' \xrightarrow{k'} B' \text{ and } A'' \xrightarrow{k''} B''$$

The mass balance demands [A] = [A′] + [A′′] and [B] = [B′] + [B′′]. That means that all further relations can be applied to the respective isotope by substitution of A, B, and *k*. The concentration of the product [B] increases as the substrate concentration decreases. At time *t* the product concentration is given by:

$$[B_t] = [A_0] - [A_t] \qquad (Eq.\ 3)$$

The reaction rate of the pseudo first-order reaction depends on the concentration of the substrate:

$$d[A_t]/dt = -k \cdot [A_t]$$
$$[A_t]/[A_0] = exp(-k \cdot t) \qquad (Eq.\ 4)$$

The total reaction rate equals the sum of the two rate terms:

$$d[A_t]/dt = d[A_t']/dt + d[A_t'']/dt$$
$$[A_t] \cdot k = [A_t'] \cdot k' + [A_t''] \cdot k''$$

At any time in the course of the reaction, the ^{12}C abundance is approximately a factor of 10^2 higher than the ^{13}C abundance, and changes in this relation occur beyond the 10^2 scale. Therefore, it was estimated that $[A''] \cdot k''$ was small compared with $[A'_t] \cdot k'$ and could be excluded from further consideration. This approximation yields the following relation:

$$k = k' \qquad (Eq.\ 5)$$

The fraction of reaction is given by the amount of B formed during the course of the reaction. It was normalized by the final concentration of the product [B_∞], which equates to the starting concentration of the substrate [A_0].

$$f = [B_t]/[A_0] \qquad (Eq.\ 6)$$

$$f = 1 - [A_t]/[A_0] \qquad \text{with equation 3}$$
$$f = 1 - exp(-k \cdot t) \qquad \text{with equation 4} \qquad (Eq.\ 7)$$

From this, an expression for time *t* is derived:

$$t = -log(1 - f)/k$$
$$t = -log(1 - f)/k' \quad \text{with equation 5} \qquad (Eq.\ 8)$$

By combining equations 6, 7, and 8 the product concentration is given by:

$$[B_t] = (1 - exp(-k \cdot (-log(1 - f)/k'))) \cdot [A_0] \qquad (Eq.\ 9)$$

The isotopic ratio of the product is defined as the quotient of the concentrations of the heavier and the lighter isotopes:

$$R_t = [B_t'']/[B_t'] \qquad (Eq.\ 10)$$

Yet another approximation took into account that in practice, the calculation of the fraction of reaction *f* was afflicted with errors that would exceed deviations between the *f*s:

$$f = f' = f'' \qquad (Eq.\ 11)$$

By adapting equation 9 to the different isotopes and insertion into equation 10 we obtain:

$$R_t = \frac{1 - exp(-k'' \cdot (-log(1 - f)/k'))}{1 - exp(-k' \cdot (-log(1 - f)/k'))} \cdot \frac{[A_0'']}{[A_0']} \qquad (Eq.\ 12)$$

The quotient $[A_0'']/[A_0']$ corresponds to the isotopic ratio of the product after complete reaction, referred to as R_∞. The rate constants can be substituted using the definition $\alpha = (k'/k'')$. Thereby R_t can be expressed as a function of *f* with the two parameters α and R_∞:

$$R_t = \frac{1 - exp(log(1 - f)/\alpha)}{f} \cdot R_\infty \qquad (Eq.\ 13)$$

REFERENCES

1. Cleland, W. W. 1982. Use of isotope effects to elucidate enzyme mechanisms. *CRC Crit. Rev. Biochem.* **13:** 385–428.
2. O'Leary, M. H. 1981. Carbon isotope fractionation in plants. *Phytochemistry.* **20:** 553–567.
3. Hayes, J. M. 2001. Fractionation of the Isotopes of Carbon and Hydrogen in Biosynthetic Processes. Vol. 43. Mineralogical Society of America, Washington DC. 225–277.
4. Niro, M. J. D., and S. Epstein. 1977. Mechanism of carbon isotope fractionation associated with lipid synthesis. *Science.* **197:** 261–263.
5. Melzer, E., and H-L. Schmidt. 1987. Carbon isotope effects on the pyruvate dehydrogenase reaction and their importance for relative carbon-13 depletion in lipids. *J. Biol. Chem.* **262:** 8159–8164.
6. Flenker, U., U. Güntner, and W. Schänzer. 2008. ^{13}C-values of endogenous urinary steroids. *Steroids.* **73:** 408–416.
7. Goldstein, J. L., and M. S. Brown. 1990. Regulation of the mevalonate pathway. *Nature.* **343:** 425–430.
8. Istvan, E. S., M. Palnitkar, S. K. Buchanan, and J. Deisenhofer. 2000. Crystal structure of the catalytic portion of human HMG-CoA reductase: insights into regulation of activity and catalysis. *EMBO J.* **19:** 819–830.
9. Chatterjee, S., J. Schoepe, S. Lohmer, and D. Schomburg. 2005. High level expression and single-step purification of hexahistidine-tagged l-2-hydroxyisocaproate dehydrogenase making use of a versatile expression vector set. *Protein Expr. Purif.* **39:** 137–143.
10. Mayer, R. J. 1988. Purification and properties of the catalytic domain of human 3-hydroxy-3-methylglutaryl-CoA reductase expressed in Escherichia coli. *Arch. Biochem. Biophys.* **267:** 110–118.
11. Bertani, G. 1951. Studies on lysogenesis. I. The mode of phage liberation by lysogenic Escherichia coli. *J. Bacteriol.* **62:** 293–300.
12. Bradford, M. M. 1976. A rapid and sensitive method for the quantitation of microgram quantities of protein utilizing the principle of protein-dye binding. *Anal. Biochem.* **72:** 248–254.
13. Edwards, P. A., D. Lemongello, and A. M. Fogelman. 1979. Improved methods for the solubilization and assay of hepatic 3-hydroxy-3-methylglutaryl coenzyme A reductase. *J. Lipid Res.* **20:** 40–46.
14. Saini, G. S., T. A. Wani, A. Gautam, B. Varshney, T. Ahmed, K. S. Rajan, K. K. Pillai, and J. K. Paliwal. 2006. Validation of the LC-MS/MS method for the quantification of mevalonic acid in human plasma and determination of the matrix effect. *J. Lipid Res.* **47:** 2340–2345.
15. Flenker, U., M. Hebestreit, T. Piper, F. Hülsemann, and W. Schänzer.

2007. Improved performance and maintenance in gas chromatography/isotope ratio mass spectrometry by precolumn solvent removal. *Anal. Chem.* **79:** 4162–4168.
16. Schimmelmann, A. H, C, N, O stable isotope reference materials from Indiana University, URL: http://php.indiana.edu/~aschimme/hc.html, Oct 2008.
17. Cleveland, W. S., E. Grosse, W. M. Shyu. Local Regression Models. *In* Chambers, J. M., and T. J. Hastie, editors. 1992. Statistical Models. S. Wadsworth & Brooks/Cole Computer Science, Pacific Grove, CA. Chapter 8.
18. Wu, J. T., L. H. Wu, and J. A. Knight. 1986. Stability of NADPH: effect of various factors on the kinetics of degradation. *Clin. Chem.* **32:** 314–319.
19. R Development Core Team. 2008. R: A Language and Environment for Statistical Computing. R Foundation for Statistical Computing, Vienna, Austria.
20. Huber, P. J. 1981. Robust Statistics. John Wiley & Sons, Inc., New York.
21. Carpenter, J., and J. Bithell. 2000. Bootstrap confidence intervals: when, which, what? A practical guide for medical statisticians. *Stat. Med.* **19:** 1141–1164.
22. O'Leary, M. H., H. Yamada, and C. J. Yapp. 1981. Multiple isotope effect probes of glutamate decarboxylase. *Biochemistry.* **20:** 1476–1481.
23. Rosenberg, R. M., and M. H. O'Leary. 1985. Aspartate (beta)-decarboxylase from Alcaligenes faecalis: carbon-13 kinetic isotope effect and deuterium exchange experiments. *Biochemistry.* **24:** 1598–1603.
24. Melzer, E., and H-L. Schmidt. 1988. Carbon isotope effect on the decarboxylation of carboxylic acids—comparison of the lactate oxidase reaction and the degradation of pyruvate by H2O2. *Biochem. J.* **252:** 913–915.
25. Tong, J. Y., and P. E. Yankwich. 1957. Calculation of experimental isotope effects for pseudo first-order irreversible reactions. *J. Phys. Chem.* **61:** 540–543.
26. O'Leary, M. H. 1980. Determination of heavy-atom isotope effects on enzyme-catalysed reactions. *Methods Enzymol.* **64:** 83–104.
27. Monson, K. D., and L. M. Hayes. 1982. Carbon isotopic fractionation in the biosynthesis of bacterial fatty acids. Ozonolysis of unsaturated fatty acids as a means of determining the intramolecular distribution of carbon isotopes. *Geochim. Cosmochim. Acta.* **46:** 139–149.
28. WADA Laboratory Committee. 2004. Reporting and Evaluation Guidance for Testosterone, Epitestosterone, T/E Ratio and Other Endogenous Steroids. World Anti Doping Agency, Montreal, WADA document TD2004EAAS.
29. Craig, H. 1953. The geochemistry of the stable carbon isotopes. *Geochim. Cosmochim. Acta.* **3:** 53–92.